

A glimpse into the future: the 2023 ocean temperature and sea-ice extremes in the context of longer-term climate change

Article

Published Version

Creative Commons: Attribution 4.0 (CC-BY)

Open Access

Kuhlbrodt, T. ORCID: <https://orcid.org/0000-0003-2328-6729>,
Swaminathan, R. ORCID: <https://orcid.org/0000-0001-5853-2673>, Ceppi, P. and Wilder, T. ORCID: <https://orcid.org/0000-0002-1108-4655> (2024) A glimpse into the future: the 2023 ocean temperature and sea-ice extremes in the context of longer-term climate change. *Bulletin of the American Meteorological Society*, 105 (3). E474-E485. ISSN 1520-0477 doi: 10.1175/BAMS-D-23-0209.1 Available at <https://centaur.reading.ac.uk/114727/>

It is advisable to refer to the publisher's version if you intend to cite from the work. See [Guidance on citing](#).

To link to this article DOI: <http://dx.doi.org/10.1175/BAMS-D-23-0209.1>

Publisher: American Meteorological Society

www.reading.ac.uk/centaur

CentAUR

Central Archive at the University of Reading

Reading's research outputs online

A Glimpse into the Future

The 2023 Ocean Temperature and Sea Ice Extremes in the Context of Longer-Term Climate Change

Till Kuhlbrodt[✉], Ranjini Swaminathan, Paulo Ceppi, and Thomas Wilder

KEYWORDS:
North Atlantic
Ocean;
Sea ice;
Southern Ocean;
Extreme events;
Sea surface
temperature;
Radiation budgets

ABSTRACT: In the year 2023, we have seen extraordinary extrema in high sea surface temperature (SST) in the North Atlantic and in low sea ice extent in the Southern Ocean, outside the 4σ envelope of the 1982–2011 daily time series. Earth's net global energy imbalance (12 months up to September 2023) amounts to $+1.9 \text{ W m}^{-2}$ as part of a remarkably large upward trend, ensuring further heating of the ocean. However, the regional radiation budget over the North Atlantic does not show signs of a suggested significant step increase from less negative aerosol forcing since 2020. While the temperature in the top 100 m of the global ocean has been rising in all basins since about 1980, specifically the Atlantic basin has continued to further heat up since 2016, potentially contributing to the extreme SST. Similarly, salinity in the top 100 m of the ocean has increased in recent years specifically in the Atlantic basin, and in addition in about 2015 a substantial negative trend for sea ice extent in the Southern Ocean began. Analyzing climate and Earth system model simulations of the future, we find that the extreme SST in the North Atlantic and the extreme in Southern Ocean sea ice extent in 2023 lie at the fringe of the expected mean climate change for a global surface-air temperature warming level (GWL) of 1.5°C , and closer to the average at a 3.0°C GWL. Understanding the regional and global drivers of these extremes is indispensable for assessing frequency and impacts of similar events in the coming years.

<https://doi.org/10.1175/BAMS-D-23-0209.1>

Corresponding author: Till Kuhlbrodt, t.kuhlbrodt@reading.ac.uk

In final form 16 December 2023

© 2024 American Meteorological Society. This published article is licensed under  the terms of a Creative Commons Attribution 4.0 International (CC BY 4.0) License

As the months of June–November 2023 were declared the hottest on record since 1880, when global records began (Ripple et al. 2023; ECMWF 2023b), attention has focused on the oceans, which cover 71% of the Earth's surface and whose uptake of heat and carbon is crucial in mitigating global heating. We discuss here two key record-breaking phenomena associated with this ocean warming (Met Office 2023). First, since March 2023 the North Atlantic Ocean sea surface temperature (SST) has been at its warmest since at least 1900, and most likely for much longer than that. Second, since May 2023 the sea ice extent in the Southern Ocean has been the smallest since the records began in 1979. While the SST and sea ice extent extremes are still developing at the time of writing, here we attempt a first analysis of longer-term, large-scale drivers: Earth's energy imbalance (EEI) and trends in the subsurface ocean. We also put the current extremes into the context of simulated future global warming levels.

North Atlantic SST and Southern Ocean sea ice extent

As of August 2023, the North Atlantic was about 1.4°C warmer than the 1982–2011 average (Fig. 1a), and this value lies substantially outside the 2σ envelope. Indeed, both in July and

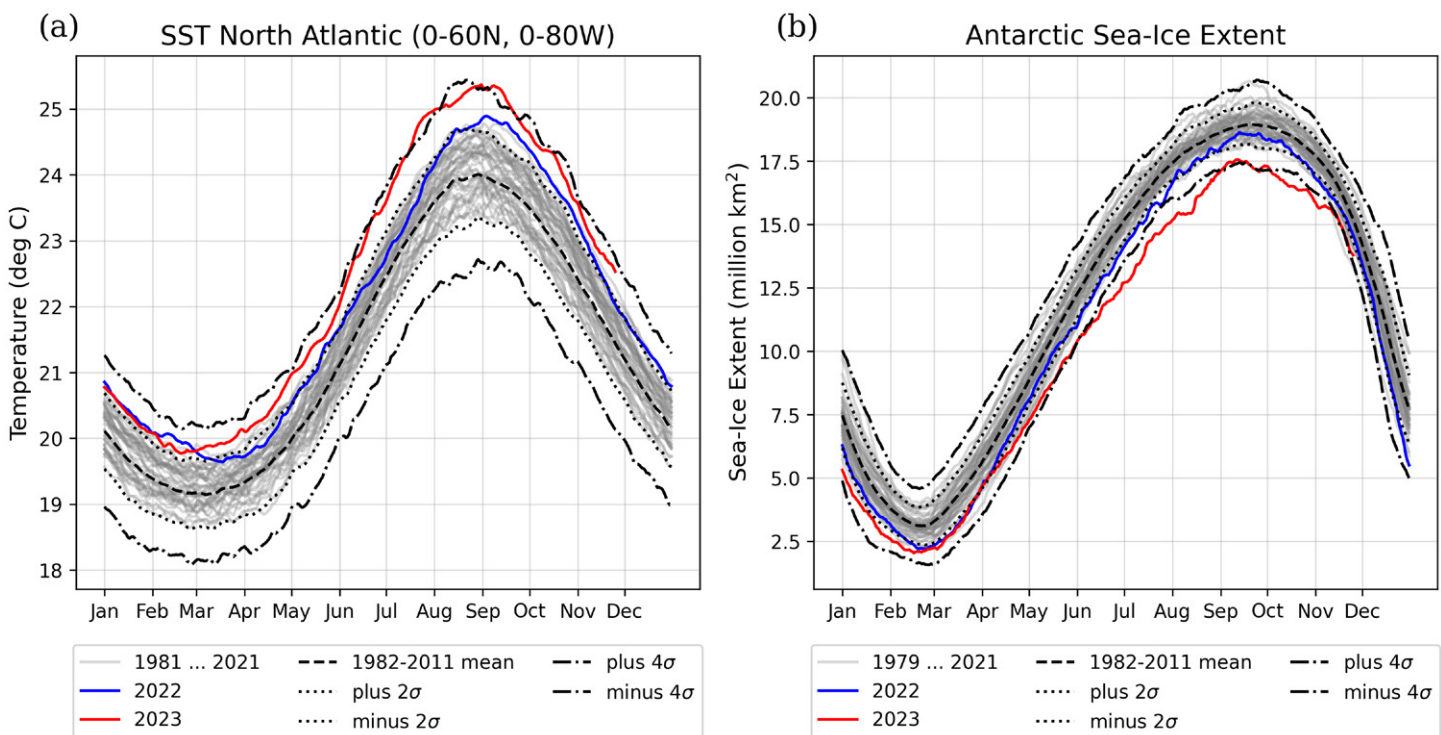


Fig. 1. Daily data of (a) North Atlantic sea surface temperature and (b) Antarctic sea ice extent. Sea surface temperature is from the NOAA OI SST V2 High Resolution Dataset provided by the NOAA Physical Sciences Laboratory (<https://psl.noaa.gov>), with details in Huang et al. (2021). For the North Atlantic we averaged over the domain 0°–60°N and 0°–80°W. Antarctic sea ice extent from EUMETSAT OSI SAF (2023). The σ stands for standard deviation.

September 2023 North Atlantic SST was outside the 4σ envelope for a couple of weeks. In other words, in these two months of 2023 the observations were four standard deviations larger than the 1982–2011 average. Before 2023, even the warmest year since 1981 was only about 0.8°C , or 2σ , above that average, illustrating the extreme scale of this warming event.

The sea ice extent in the Southern Ocean (Fig. 1b) is similarly extreme as the North Atlantic SST. For August 2023, Antarctic sea ice extent was about 2.4 million km^2 smaller than the 1981–2011 average, and this value, as the ones for July and October, lies outside the 4σ envelope. From May all the way into November, Southern Ocean sea ice extent was close to the 4σ curve.

In the following we discuss the role of Earth's energy imbalance as a global driver for these extremes, and we consider several potential regional drivers. We then set Atlantic temperatures in the context of the global ocean by exploring indications for the Atlantic Ocean, here understood as the entire basin stretching from the Arctic Ocean to the Weddell Sea, having different temperature signals than the other basins, and showing signs for a connection between the North Atlantic and the Southern Ocean extremes.

Earth's energy imbalance

Anthropogenic forcing, predominantly from greenhouse gas emissions, drives a positive EEI, reflecting an accumulation of energy that results in global warming. Around 91% of this extra energy is taken up by the ocean (Forster et al. 2021; Fig. 3c). The Intergovernmental Panel on Climate Change's sixth assessment report evaluated the EEI at $0.79 \pm 0.27 \text{ W m}^{-2}$ for the period 2006–18 (Forster et al. 2021), while a similar value of $0.76 \pm 0.2 \text{ W m}^{-2}$ was reported by von Schuckmann et al. (2023) for the period 2006–20. The EEI is steadily growing, however, as a result of an increasing radiative forcing; the most recent assessment for the period 2010–22 reports an EEI of $0.89 \pm 0.26 \text{ W m}^{-2}$ (Forster et al. 2023).

An analysis of the latest global satellite observations of EEI (Fig. 2) confirms the rapid growth in EEI. As of the 2022 annual mean, the imbalance reached around $+1.5 \text{ W m}^{-2}$, much higher than the numbers reported in recent assessments; as of the most recent available 12-month period October 2022–September 2023, this imbalance had risen even further to $+1.9 \text{ W m}^{-2}$. Much of this rapid increase is likely to be driven by natural climate variability (Palmer and McNeall 2014); for instance, extra radiative heating is expected during the growing phase of El Niño

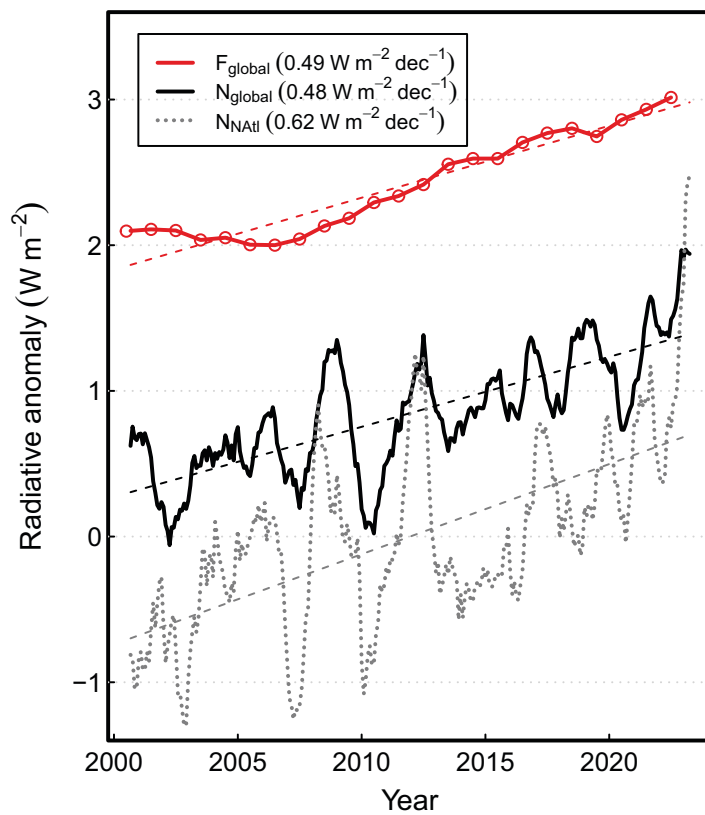


Fig. 2. CERES EBAF (Loeb et al. 2018) net radiative imbalance (positive down, 12-month running means), March 2000–September 2023 for the whole Earth (N_{global} ; black, solid) and the North Atlantic (N_{NAtl} ; black, dotted), and annual-mean effective radiative forcing (F_{global} from Forster et al. 2023; red) up to 2022. For visualization purposes, an arbitrary offset was added to the North Atlantic net radiative imbalance such that the time series averages out to zero.

(Ceppi and Fueglistaler 2021). Note that the Clouds and Earth's Radiant Energy Systems (CERES) product provides no error estimates for interannual variations in the EEI.

Although there is considerable interannual variability in the time series of global-mean net radiative imbalance in Fig. 2, Loeb et al. (2021) and von Schuckmann et al. (2023) demonstrate the close match between the EEI estimates from the CERES Energy Balanced and Filled (EBAF) product and from global ocean heat content (OHC) change, thus corroborating the large positive trend. Radiative forcing from increasing concentrations of greenhouse gases and from other forcing agents (e.g., less negative aerosol forcing from implemented emissions reductions), not shown here, all contribute to the upward trend in effective radiative forcing.

Potential regional atmospheric drivers

It has been suggested that a reduction in negative aerosol radiative forcing from reduced advection of Saharan dust, or from reduced emissions from ships combusting fossil fuel (Diamond 2023), has led to a net increase in positive radiative forcing over the North Atlantic, and thus contributed to the current SST extremes. Given the interannual variability of EEI it is not possible to identify a weakened negative aerosol forcing [globally on the order of 0.1 W m^{-2} as estimated by Diamond (2023)] over the North Atlantic or Earth as a whole (dotted and solid black in Fig. 2) since 2020, when an international agreement on reducing ship emissions came into force. A closer examination of the individual contributors to the year-by-year variability of the net radiative imbalance is required here.

Apart from radiative anomalies, other regional drivers could include changes in atmospheric circulation, and associated anomalies in heat and momentum fluxes between the ocean and atmosphere (Dai et al. 2015). Initial analyses have pointed to various atmospheric drivers of the observed SST and sea ice extremes, including a weaker Azores high, a developing El Niño, and the position of atmospheric lows in the Southern Ocean (Met Office 2023; ECMWF 2023a). The pattern of amplified SST warming in the North and South Atlantic midlatitudes (Figs. 5 and 6 below) hints at some role for changes in the strength and position of the jet streams in both hemispheres—possibly projecting onto the Atlantic multidecadal variability for the North Atlantic—in driving the observed warming and salinification patterns that we discuss below.

Of the drivers discussed so far, it seems very likely that the substantial positive trend in the twenty-first-century EEI leads to a larger likelihood for temperature extremes as in 2023. The role of El Niño as a driver for the extremes in the North Atlantic and the Southern Ocean needs further study; we note that the onset of these extremes in the first few months of 2023 occurs about 8 or 9 months earlier than the expected maximum of the 2023/24 El Niño. Regional atmospheric forcing, e.g., through wind stress changes, is probably a major driver.

Potential oceanic precursors

Simple heat budget considerations show that temperature (or heat content) anomalies in the ocean's surface layer must result from a combination of changes in surface heat fluxes and in three-dimensional heat transport divergence. After having discussed surface heat flux in the preceding sections, we now investigate internal ocean heat transport. In particular, given the large magnitude of the North Atlantic and Southern Ocean extremes (Fig. 1), we seek oceanic precursors for these extremes. First, we analyze 3-monthly mean basin time series of vertical mean temperature and salinity anomaly from NCEI (Levitus et al. 2012), which are based on in situ data and come with basinwide estimates of the observational uncertainty. Specifically, we analyze the January–March means for the average of the uppermost 100 m.

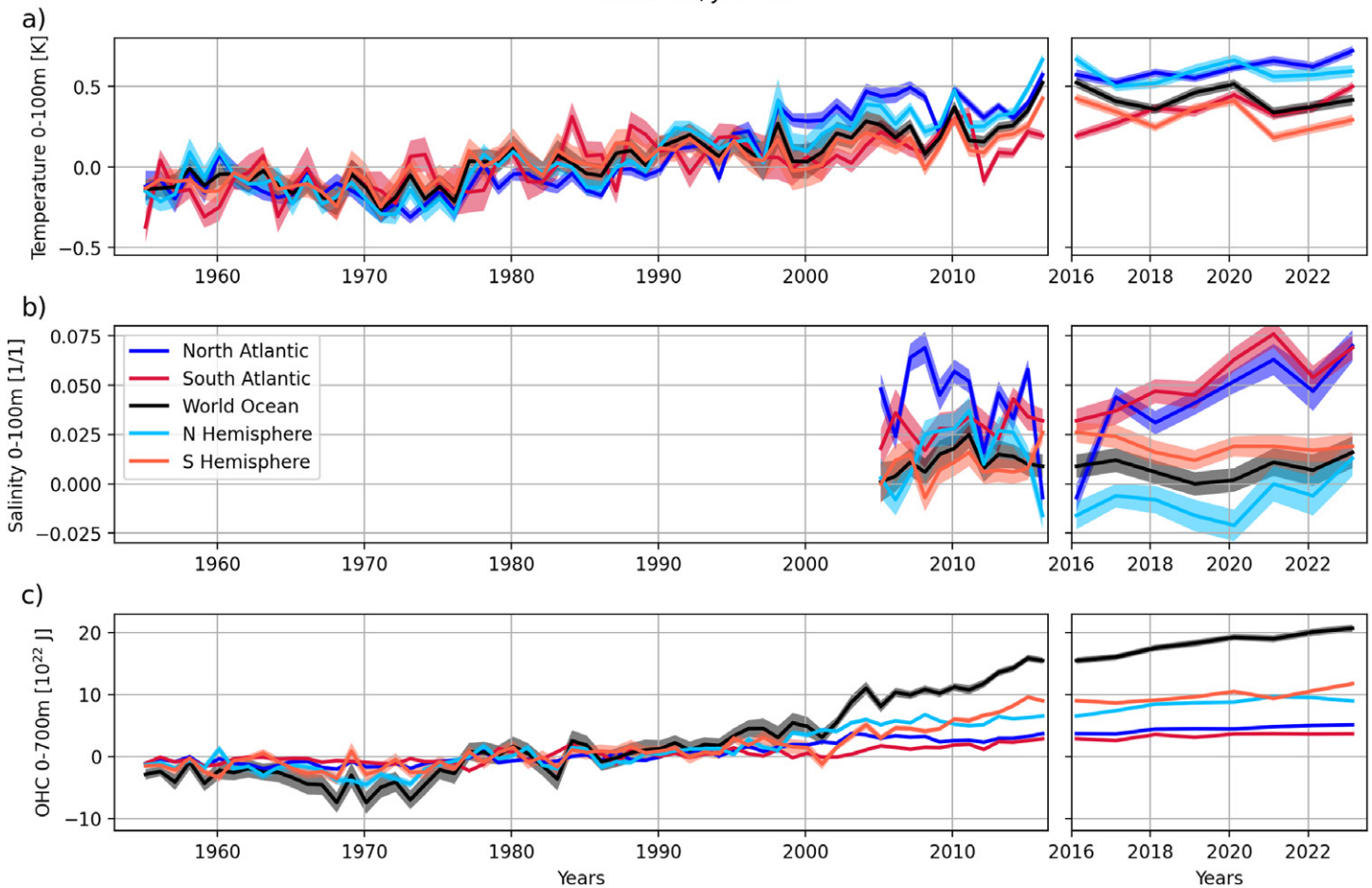


Fig. 3. NCEI data, January–March averages. (a) Ocean temperature anomalies (0–100-m average) 1955–2023. (b) Salinity anomalies (0–100-m average) 2005–23. (c) Ocean heat content anomalies 1955–2023 in the top 700m. For all panels, the reference period is 1955–2006, and the shading indicates the observational uncertainty. Panels in the right column are a close-up for the years since 2016.

Figure 3a illustrates the pronounced warming trend since about 2000 for all ocean basins (see the appendix for details on the basin definitions used here) in the uppermost 100 m. But since 2016 only the North and South Atlantic Ocean (dark blue and dark red curves in the right-hand panel of Fig. 3a) have warmed, while the global ocean and both hemispheres have slightly cooled (other curves in Fig. 3a).

We acknowledge that uncertainty estimates for any one individual observational dataset probably underestimate the actual, or total uncertainty (Palmer et al. 2021). Therefore, we look at a different dataset (EN4.2.2; Good et al. 2013) which has the additional benefit of stretching much further into the past. The EN4.2.2 time series of 0–100-m temperature (Fig. 4) confirm the long-term and recent warming trends specifically for the Atlantic basin. We suggest that these trends and all-time high temperature in the top 100 m of the North Atlantic in January–March 2023 are very likely contributing to the SST extrema of the boreal summer 2023. [For the equivalent of Fig. 3 using April–June means (not shown) the picture is different since in those 3 months the extreme SST was already manifest.]

In the 2000s there was a multiyear episode of the North Atlantic being about 0.2 K warmer than the other basins. This could be interpreted as multiannual variability playing a role for extrema, including the current ones. There could also be a role for a positive cloud–SST feedback (Boehm and Thompson 2023) contributing to the current North Atlantic heat through its role in amplifying SST variability.

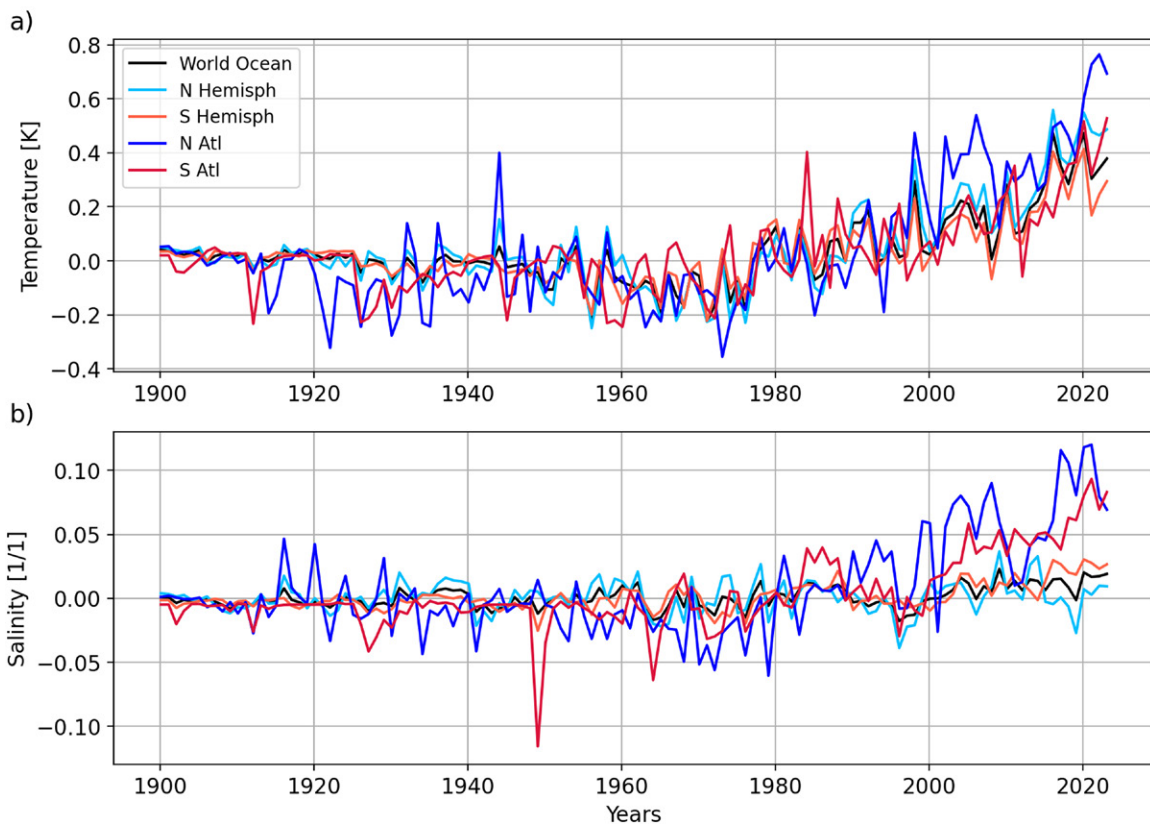


Fig. 4. (a) Temperature and (b) salinity anomalies, averaged over the top 100m for January–March of each year, from EN4.2.2 (Good et al. 2013) using expendable bathythermograph (XBT) corrections (Cheng et al. 2014) and mechanical bathythermograph (MBT) corrections (Gouretski and Cheng 2020). The reference period is 1955–2006.

Salinity changes, lacking temperature's direct coupling to the atmosphere, can indicate large-scale and longer-term changes in the ocean's circulation and freshwater budget. In salinity averaged across the top 100 m (Fig. 3b), we see that, similarly to Fig. 3a, the whole Atlantic basin has become more saline since about 2016, while there is no such trend for the global ocean and its two hemispheric parts. Taking longer observation-based salinity time series into account (Fig. 4b), we see that since the early 2000s the average 0–100-m salinity has increased substantially faster in the Atlantic basins than in the World Ocean as a whole (Aretxabaleta et al. 2017), establishing a larger salinity contrast between the Atlantic and the Indo-Pacific basins. These specific salinity trends in the Atlantic, together with the temperature trends discussed above, certainly warrant a closer analysis of their contribution to the current extremes. For instance, Zhu et al. (2023) see an increased SSS contrast between the subtropical Atlantic and Indo-Pacific basins of the Southern Hemisphere as an indication of a weakening of the Atlantic meridional overturning circulation (AMOC) in climate model simulations. Available observations up to 2016 from the RAPID array in the North Atlantic do not show signals of a weakening AMOC though (Worthington et al. 2021). Current observations of the AMOC from these arrays will have to be read from the in situ instruments and therefore are unavailable at the time of writing.

The time series of 3-monthly mean ocean heat content (OHC) in the top 700 m (Fig. 3c) provide a different picture compared to the temperature in the 0–100-m layer (cf. Allison et al. 2020). For 2023 we see an all-time high (at least since 1955) in the global ocean, in the Southern Hemisphere, in the Atlantic as a whole, and in the North Atlantic. The OHC in the top 700 m does not show the specific features of the average temperature in the top 100 m.

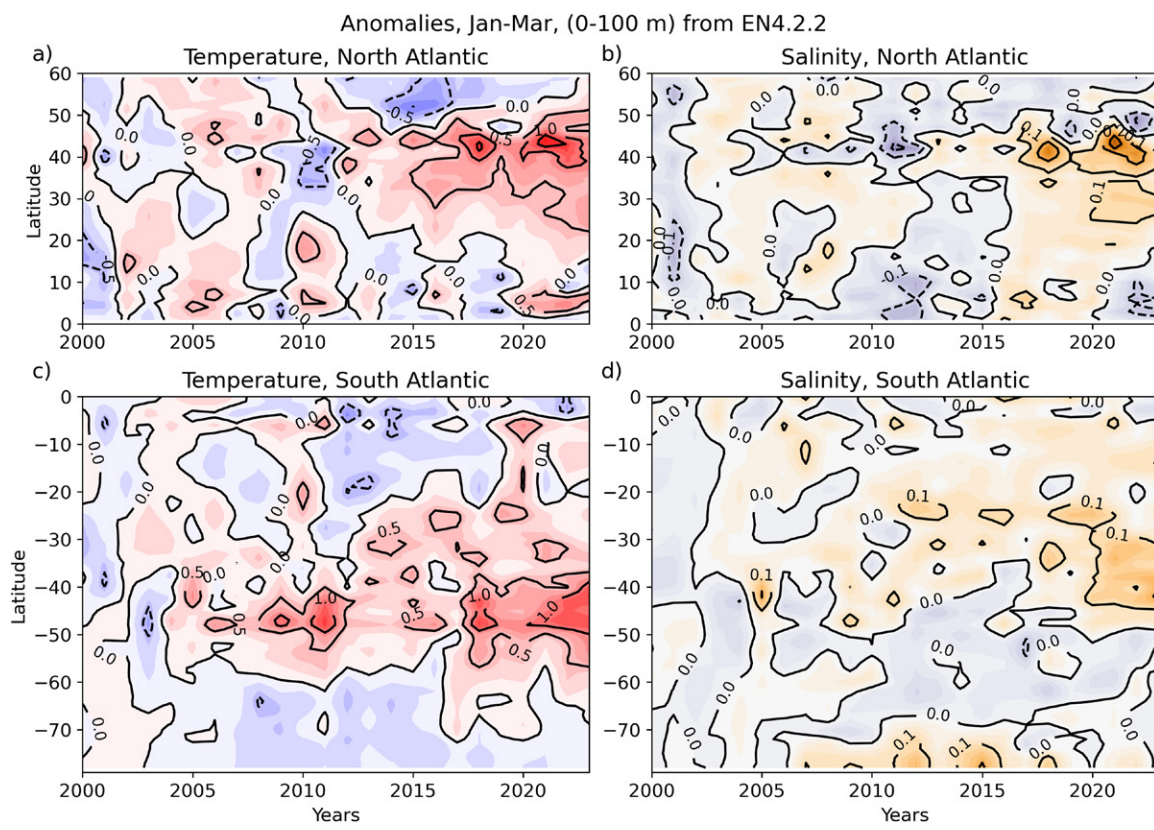


Fig. 5. Hovmöller plot of (a),(c) temperature (K) and (b),(d) salinity (dimensionless) anomalies in the two Atlantic basins, from the same EN4.2.2 dataset as in Fig. 4. Reference period 2000–06.

In other words, the warming of the top 100 m in the Atlantic, specifically since 2016, must be confined to the top few hundred meters at most.

Patterns of warming and salinification

The anomalies for the North and South Atlantic basins as a function of time and latitude (Fig. 5) reveal that in both basins the twenty-first-century temperature trends are strongest between 40° and 50° latitude, especially since about 2015 in the North Atlantic and since about 2005 in the South Atlantic. Since about 2010 there are also discernible upward temperature trends in the subtropical regions of the South Atlantic. In the North Atlantic, salinity trends are strongest in the same midlatitude band as the temperature, and again since about 2015, while in the South Atlantic the salinity anomalies are strongest in the subtropical latitudes and in the Weddell Sea, poleward of 70°S. Note that the warm anomalies in the midlatitude North Atlantic appear to be largely density compensated by positive salinity anomalies (e.g., Menary et al. 2015) while the warm anomalies in the South Atlantic are not density compensated.

The full spatial pattern of the extreme SSTs (Fig. 6) from a NASA dataset (Lenssen et al. 2019) shows that in June 2023 [and in the preceding months (not shown)] the North Atlantic warming occurred mostly in the eastern half of the basin with a focus on the midlatitude and the tropics. For the high-latitude Southern Ocean, near-real-time temperature observations are lacking because of the sea ice cover in austral winter. Nevertheless, based on a few temperature observations from land-based and ice-sheet-based stations, Fig. 6 shows that the western and southern coasts of the Weddell Sea are very warm in comparison to the 1981–2021 mean, while there is a cold anomaly over the Amundsen Sea. This pattern corroborates the hypothesis of a strong Amundsen Sea low since that implies advection of warmer air from

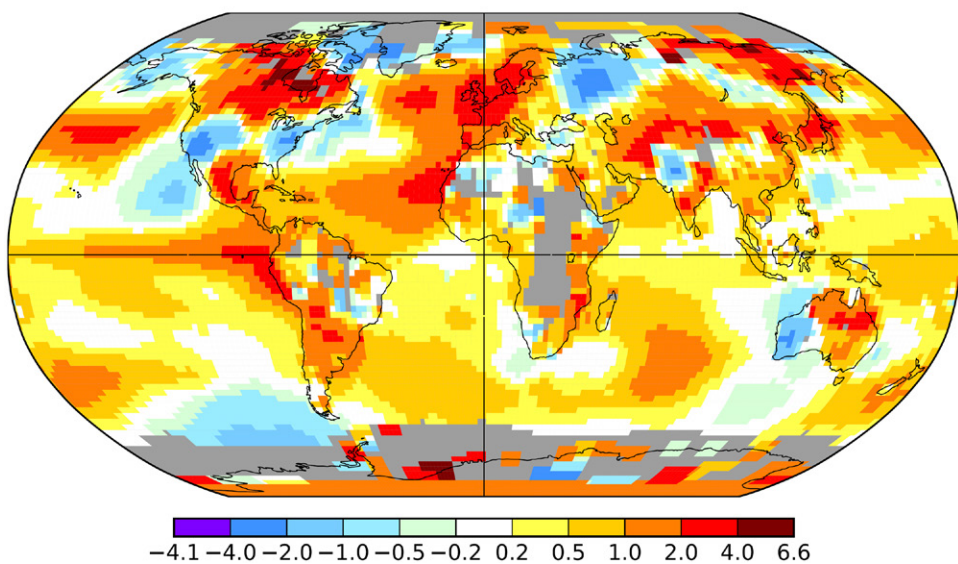


Fig. 6. NASA land–ocean temperature index (L-OTI) for June 2023 (GISTEMP Team 2023). L-OTI maps show SAT anomalies over land and sea ice and SST anomalies over (ice-free) water.

the north over the Weddell Sea, and advection of colder air from the Antarctic continent onto the Amundsen Sea (ECMWF 2023c).

Southern Ocean sea ice

The extremely small sea ice extent in 2023 (Fig. 1) is a continuation of the recent trend reversal in Antarctic sea ice extent (Fig. 7). While the June Antarctic sea ice extent followed an upward trend of around $0.26\% \text{ yr}^{-1}$ from 1979 to 2014, since about 2014 this trend has reversed and is now negative, decreasing by $1.76\% \text{ yr}^{-1}$. The magnitude of this trend is also notably larger than before (Fetterer et al. 2017). The June 2023 extreme value is consistent with this recent downward trend of the past 9 years. The upward trend in Southern Atlantic temperature in the top 100 m (Fig. 3a) since 2016 will very likely be closely linked with the downward trend in sea ice extent (Purich and Doddridge 2023). It is tempting to speculate whether the global ocean circulation links the substantial trend changes in Southern Ocean sea ice extent around 2015 (Fig. 7) and in North Atlantic temperature and salinity (0–100 m; Fig. 3) much around the same time.

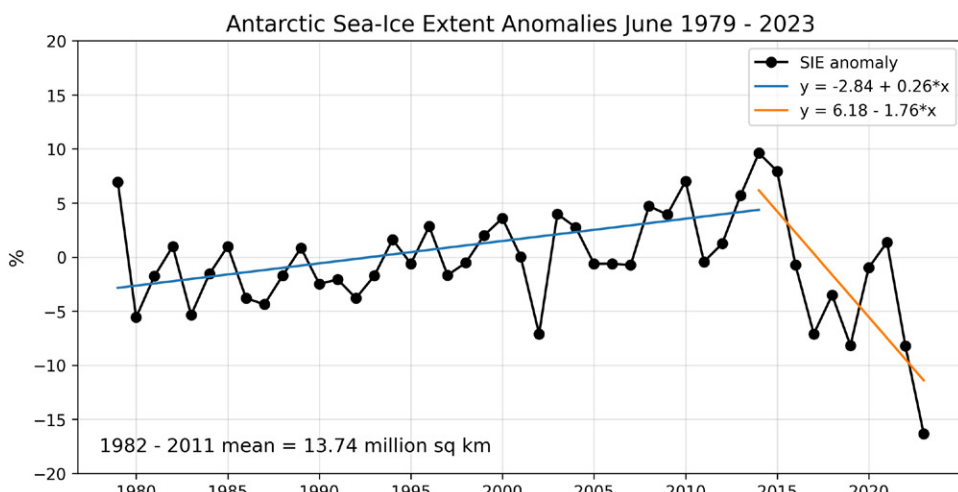


Fig. 7. Antarctic sea ice extent anomalies in June for the period 1979–2023 against a baseline mean 1982–2011. Data acquired from EUMETSAT OSI SAF (2023).

Changes at global warming levels

Assessments of the state of the climate at different global surface air temperature warming levels (GWL) such as at 1.5°C allow us to study the impacts of anthropogenic warming on different components of the Earth system and how they may be interconnected, especially for effective policy formulation around adaptation and mitigation (Tebaldi et al. 2021; Arias et al. 2023). Analyzing ensemble simulations of future climate evolution guides us on whether and when the currently observed extremes in North Atlantic SST and Antarctic sea ice cover are to be expected as a result of the continuously increasing greenhouse gas concentrations and their impact on the global climate. We follow Swaminathan et al. (2022) in their approach of calculating the years of GWL exceedance, defined by global surface air temperature change with respect to the period 1850–1900.

We calculate the 21-yr *mean* changes in the North Atlantic SST and Antarctic sea ice extent centered around the year when different GWLs such as 1.5°, 2.0°, 3.0°, 4.0°, and 5.0°C are exceeded compared to the 1982–2011 *mean* June–August (JJA) climatology. (By construction this approach gives no information about the distribution of values in a particular year.) This gives us expected ranges of changes seen in the two quantities at different GWLs in the future, allowing us to place current observations in the context of estimated future changes in an illustrative way.

Five different future Shared Socioeconomic Pathway (SSP) scenarios are considered, including all Tier 1 SSPs (1–1.9, 1–2.6, 2–4.5, 3–7.0, and 5–8.5), from Earth system models (ESMs) in the phase 6 of the Coupled Model Intercomparison Project (CMIP6) for our analysis (Andela et al. 2023a,b; Cinquini et al. 2014). Data from 28 and 8 CMIP6 models, listed in Table 1, were used for North Atlantic SST change and Antarctic sea ice extent change analysis, respectively, as shown in Fig. 8. Beginning with the sea ice extent, the top-left blue triangle in Fig. 8 signifies that the 21-yr mean sea ice extent loss around a GWL of 1.5°C (horizontal scale) in the ensemble of the CMIP6 SSP simulations is 0.7 million km² (right-hand scale). However, referring to Fig. 1 we see that the current loss of sea ice extent amounts to roughly 2.4 million km² (seen as a blue dashed line in Fig. 8). In the CMIP6 SSP ensemble a sea ice loss of this extent is expected for the ensemble-average conditions at a GWL of 3.0°C. In other words, the 2023 conditions in the high-latitude Southern Ocean provide a glimpse of what the *average* conditions will be at a 3.0°C GWL, using interpolation on this eight-model ensemble.

Table 1. CMIP6 models and corresponding ensemble members used in the analysis shown in Fig. 8. All models listed were used to calculate the North Atlantic SST changes; models with an asterisk were used in the calculation of Antarctic sea ice change at different GWLs.

No.	Used for sea ice	Model	Ensemble member
1	*	ACCESS-CM2	r1i1p1f1
2	*	ACCESS-ESM1-5	r1i1p1f1
3		BCC-CSM2-MR	r1i1p1f1
4		CanESM5	r1i1p2f1
5		CESM2-WACCM	r1i1p1f1
6		CIESM	r1i1p1f1
7		CMCC-CM2-SR5	r1i1p1f1
8		CMCC-ESM2	r1i1p1f1
9		CNRM-CM6-1-HR	r1i1p1f2
10		CNRM-ESM2-1	r1i1p1f2
11	*	EC-Earth3	r1i1p1f1
12	*	EC-Earth3-Veg	r1i1p1f1
13		FGOALS-f3-L	r1i1p1f1
14		FGOALS-g3	r1i1p1f1
15		FIO-ESM-2-0	r1i1p1f1
16		GFDL-ESM4	r1i1p1f1
17	*	GISS-E2-1-G	r1i1p1f2
18		INM-CM4-8	r1i1p1f1
19		IPSL-CM6A-LR	r1i1p1f1
20		MCM-UA-1-0	r1i1p1f2
21		MIROC-ES2L	r1i1p1f2
22		MIROC6	r1i1p1f1
23	*	MPI-ESM1-2-LR	r1i1p1f1
24	*	MRI-ESM2-0	r1i1p1f1
25		NorESM2-LM	r1i1p1f1
26		NorESM2-MM	r1i1p1f1
27	*	UKESM1-0-LL	r1i1p1f2
28		TaiESM1	r1i1p1f1

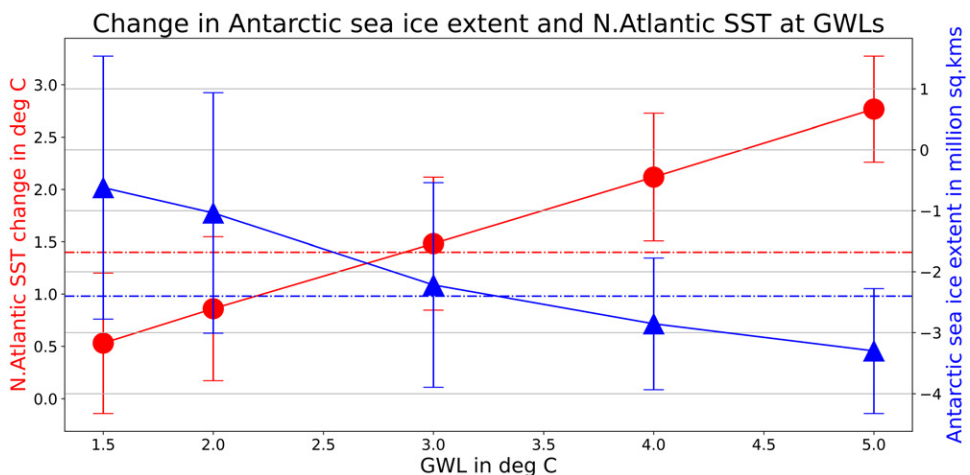


Fig. 8. Analysis of changes in the North Atlantic sea surface temperature and Antarctic sea ice extent at different GWLs in CMIP6 models. Changes in North Atlantic SST ($^{\circ}\text{C}$) in red circles (left-hand scale) and changes in Antarctic sea ice extent (10^6 km^2) in blue triangles (right-hand scale). Vertical bars indicate spread as one standard deviation. Compare with Fig. 12 in Swaminathan et al. (2022). The red and blue dashed lines show the North Atlantic warming and Antarctic sea ice loss observed in August 2023. All changes are calculated for the mean JJA period with respect to the 1982–2011 JJA average climatology.

Likewise, considerations for the North Atlantic SST suggest that the current conditions in the North Atlantic—with the SST 1.4°C larger than a 40-yr average—give us, again, a glimpse of the *average* estimated conditions at a 3.0°C GWL.

In terms of the uncertainty of these estimates, we see that an SST increase of 1.4°C (red dashed line in Fig. 8) lies outside the 1σ ensemble uncertainty for a 1.5°C GWL (leftmost red dot and whiskers), and thus is relatively unlikely to happen at 1.5°C GWL in this ensemble. For sea ice extent in the Southern Ocean, the ensemble uncertainty is generally larger (cf. the sizes of the blue pairs of whiskers with the red ones), therefore a change in sea ice extent like the current one does appear in a small set of models and scenarios from these 8 CMIP6 models at a 1.5°C GWL. For comparison, the current annual-mean warming of global surface air temperature is about 1.2°C .

Summary

The extraordinary magnitude of the joint SST and sea ice extent extrema in 2023 calls for a community effort to quickly identify their drivers. This is urgently required for updating impact assessments of extreme weather on ecosystems and climate services, but also for ensuring that climate and Earth system models are fit for purpose in predicting the magnitude and frequency of extremes. As a starting point for analyzing these drivers, we posit in this essay that strong multiannual and decadal trends in Atlantic Ocean temperature and salinity might contribute to these extrema through rapid warming of the ocean’s top layer, and that they could point to large-scale oceanic circulation changes.

Along with these long-term trends, for hot extremes to materialize at the ocean and land surface as experienced in much of 2023, regional atmospheric forcing is crucial, and its role needs to be analyzed in more detail. The remarkably large upward trend in Earth’s energy imbalance in combination with short-term atmospheric forcing makes hot extremes ever more likely to occur in the future, and CMIP6 model simulations of the twenty-first century suggest that what we are experiencing in 2023 will be the average conditions if we reach 3.0°C global surface air temperature increase.

Acknowledgments. We are very grateful for detailed and constructive suggestions by three anonymous reviewers. We appreciate having access to the most recent EN4.2.2 data at the Met Office Hadley Centre,

United Kingdom. TK and RS are supported by the UKRI NERC project TerraFIRMA, Grant Reference NE/W004895/1. PC is supported by the UKRI NERC Grants NE/T006250/1 and NE/V012045/1. TW is supported by the EU Horizon project ESM2025, Grant Reference 101003536.

Appendix: Ocean basin definitions

Different datasets use different geographical definitions of the North Atlantic and the other ocean basins. In the NCEI dataset (Fig. 3), the North Atlantic is defined as the part of the Atlantic that is northward of the equator, including the whole Arctic Ocean. For the data in Fig. 1, and for our analysis of the EN4.2.2 data (Fig. 4) and the CERES EBAF data (Fig. 2), the definition is 80°W – 0° and 0° – 60°N . The different definitions show the robustness of our analyses in that the results do not depend on them. The South Atlantic (Figs. 4 and 5) is here defined as 60°W – 20°E and 80°S – 0° . Northern and Southern Hemisphere refer to all parts of the World Ocean on either side of the equator.

For the NCEI data we plotted the uncertainty estimate as defined in the original dataset. For the EN4.2.2 data the uncertainties do not currently have a defined correlation structure that would allow an error estimate for large-scale area averages.

References

Allison, L. C., M. D. Palmer, R. P. Allan, L. Hermanson, C. Liu, and D. M. Smith, 2020: Observations of planetary heating since the 1980s from multiple independent datasets. *Environ. Res. Commun.*, **2**, 101001, <https://doi.org/10.1088/2515-7620/abbb39>.

Andela, B., and Coauthors, 2023a: ESMValTool (v2.9.0). Zenodo, <https://doi.org/10.5281/zenodo.8120970>.

—, and Coauthors, 2023b: ESMValCore (v2.9.0). Zenodo, <https://doi.org/10.5281/zenodo.8112684>.

Aretxabaleta, A., K. Smith, and T. Kalra, 2017: Regime changes in global sea surface salinity trend. *J. Mar. Sci. Eng.*, **5**, 57, <https://doi.org/10.3390/jmse5040057>.

Arias, P. A., and Coauthors, 2023: Technical summary. *Climate Change 2021: The Physical Science Basis*, V. Masson-Delmotte et al., Eds., Cambridge University Press, 35–144.

Boehm, C. L., and D. W. J. Thompson, 2023: The key role of cloud–climate coupling in extratropical sea surface temperature variability. *J. Climate*, **36**, 2753–2762, <https://doi.org/10.1175/JCLI-D-22-0362.1>.

Ceppi, P., and S. Fueglistaler, 2021: The El Niño–Southern Oscillation pattern effect. *Geophys. Res. Lett.*, **48**, e2021GL095261, <https://doi.org/10.1029/2021GL095261>.

Cheng, L., J. Zhu, R. Cowley, T. Boyer, and S. Wijffels, 2014: Time, probe type, and temperature variable bias corrections to historical expendable bathythermograph observations. *J. Atmos. Oceanic Technol.*, **31**, 1793–1825, <https://doi.org/10.1175/JTECH-D-13-00197.1>.

Cinquini, L., and Coauthors, 2014: The Earth System Grid Federation: An open infrastructure for access to distributed geospatial data. *Future Gener. Comput. Syst.*, **36**, 400–417, <https://doi.org/10.1016/j.future.2013.07.002>.

Dai, A., J. C. Fyfe, S. P. Xie, and X. Dai, 2015: Decadal modulation of global surface temperature by internal climate variability. *Nat. Climate Change*, **5**, 555–559, <https://doi.org/10.1038/nclimate2605>.

Diamond, M. S., 2023: Detection of large-scale cloud microphysical changes within a major shipping corridor after implementation of the International Maritime Organization 2020 fuel sulfur regulations. *Atmos. Chem. Phys.*, **23**, 8259–8269, <https://doi.org/10.5194/acp-23-8259-2023>.

ECMWF, 2023a: Record-breaking North Atlantic Ocean temperatures contribute to extreme marine heatwaves. Copernicus Program, accessed 13 December 2023, <https://climate.copernicus.eu/record-breaking-north-atlantic-ocean-temperatures-contribute-extreme-marine-heatwaves>.

—, 2023b: Record warm November consolidates 2023 as the warmest year. Copernicus Program, accessed 13 December 2023, <https://climate.copernicus.eu/record-warm-november-consolidates-2023-warmest-year>.

—, 2023c: Sea ice cover for May 2023. Copernicus Program, accessed 12 December 2023, <https://climate.copernicus.eu/sea-ice-cover-may-2023>.

EUMETSAT OSI SAF, 2023: OSI SAF Sea ice index vn2.2, 1978–onwards. EUMETSAT, accessed 27 November 2023, https://doi.org/10.15770/EUM_SAF_OSI_0022.

Fetterer, F., K. Knowles, W. N. Meier, M. Savoie, and A. K. Windnagel, 2017: Sea ice index, version 3. NSIDC, accessed 27 November 2023, <https://doi.org/10.7265/N5K072F8>.

Forster, P., and Coauthors, 2021: The Earth’s energy budget, climate feedbacks, and climate sensitivity. *Climate Change 2021: The Physical Science Basis*, V. Masson-Delmotte et al., Eds., Cambridge University Press, 923–1054.

Forster, P. M., and Coauthors, 2023: Indicators of Global Climate Change 2022: Annual update of large-scale indicators of the state of the climate system and human influence. *Earth Syst. Sci. Data*, **15**, 2295–2327, <https://doi.org/10.5194/essd-15-2295-2023>.

GISTEMP Team, 2023: GISS Surface Temperature Analysis (GISTEMP), version 4. NASA GISS, accessed 21 July 2023, <https://data.giss.nasa.gov/gistemp/>.

Good, S. A., M. J. Martin, and N. A. Rayner, 2013: EN4: Quality controlled ocean temperature and salinity profiles and monthly objective analyses with uncertainty estimates. *J. Geophys. Res. Oceans*, **118**, 6704–6716, <https://doi.org/10.1002/2013JC009067>.

Gouretski, V., and L. Cheng, 2020: Correction for systematic errors in the global dataset of temperature profiles from mechanical bathythermographs. *J. Atmos. Oceanic Technol.*, **37**, 841–855, <https://doi.org/10.1175/JTECH-D-19-0205.1>.

Huang, B., C. Liu, V. Banzon, E. Freeman, G. Graham, B. Hankins, T. Smith, and H. M. Zhang, 2021: Improvements of the Daily Optimum Interpolation Sea Surface Temperature (DOISST) version 2.1. *J. Climate*, **34**, 2923–2939, <https://doi.org/10.1175/JCLI-D-20-0166.1>.

Lenssen, N. J. L., G. A. Schmidt, J. E. Hansen, M. J. Menne, A. Persin, R. Ruedy, and D. Zyss, 2019: Improvements in the GISTEMP uncertainty model. *J. Geophys. Res. Atmos.*, **124**, 6307–6326, <https://doi.org/10.1029/2018JD029522>.

Levitus, S., and Coauthors, 2012: World ocean heat content and thermosteric sea level change (0–2000 m), 1955–2010. *Geophys. Res. Lett.*, **39**, L10603, <https://doi.org/10.1029/2012GL051106>.

Loeb, N. G., and Coauthors, 2018: Clouds and the Earth’s Radiant Energy System (CERES) Energy Balanced and Filled (EBAF) top-of-atmosphere (TOA) edition-4.0 data product. *J. Climate*, **31**, 895–918, <https://doi.org/10.1175/JCLI-D-17-0208.1>.

—, G. C. Johnson, T. J. Thorsen, J. M. Lyman, F. G. Rose, and S. Kato, 2021: Satellite and ocean data reveal marked increase in Earth’s heating rate. *Geophys. Res. Lett.*, **48**, e2021GL093047, <https://doi.org/10.1029/2021GL093047>.

Menary, M. B., D. L. R. Hodson, J. I. Robson, R. T. Sutton, R. A. Wood, and J. A. Hunt, 2015: Exploring the impact of CMIP5 model biases on the simulation of North Atlantic decadal variability. *Geophys. Res. Lett.*, **42**, 5926–5934, <https://doi.org/10.1002/2015GL064360>.

Met Office, 2023: Sea surface temperatures breaking records. Met Office Official Blog, 16 June, accessed 19 September 2023, <https://blog.metoffice.gov.uk/2023/06/16/sea-surface-temperatures-breaking-records/>.

Palmer, M. D., and D. J. McNeall, 2014: Internal variability of Earth’s energy budget simulated by CMIP5 climate models. *Environ. Res. Lett.*, **9**, 034016, <https://doi.org/10.1088/1748-9326/9/3/034016>.

—, C. M. Domingues, A. B. A. Slanger, and F. Boeira Dias, 2021: An ensemble approach to quantify global mean sea-level rise over the 20th century from tide gauge reconstructions. *Environ. Res. Lett.*, **16**, 044043, <https://doi.org/10.1088/1748-9326/abdaec>.

Purich, A., and E. W. Doddridge, 2023: Record low Antarctic sea ice coverage indicates a new sea ice state. *Commun. Earth Environ.*, **4**, 314, <https://doi.org/10.1038/s43247-023-00961-9>.

Ripple, W. J., and Coauthors, 2023: The 2023 State of the Climate report: Entering uncharted territory. *BioScience*, **73**, 841–850, <https://doi.org/10.1093/biosci/biad080>.

Swaminathan, R., R. J. Parker, C. G. Jones, R. P. Allan, T. Quaife, D. I. Kelley, L. de Mora, and J. Walton, 2022: The physical climate at global warming thresholds as seen in the U.K. Earth System Model. *J. Climate*, **35**, 29–48, <https://doi.org/10.1175/JCLI-D-21-0234.1>.

Tebaldi, C., and Coauthors, 2021: Climate model projections from the Scenario Model Intercomparison Project (ScenarioMIP) of CMIP6. *Earth Syst. Dyn.*, **12**, 253–293, <https://doi.org/10.5194/esd-12-253-2021>.

von Schuckmann, K., and Coauthors, 2023: Heat stored in the Earth system 1960–2020: Where does the energy go? *Earth Syst. Sci. Data*, **15**, 1675–1709, <https://doi.org/10.5194/essd-15-1675-2023>.

Worthington, E. L., B. I. Moat, D. A. Smeed, J. V. Mecking, R. Marsh, and G. D. McCarthy, 2021: A 30-year reconstruction of the Atlantic meridional overturning circulation shows no decline. *Ocean Sci.*, **17**, 285–299, <https://doi.org/10.5194/os-17-285-2021>.

Zhu, C., Z. Liu, S. Zhang, and L. Wu, 2023: Likely accelerated weakening of Atlantic overturning circulation emerges in optimal salinity fingerprint. *Nat. Commun.*, **14**, 1245, <https://doi.org/10.1038/s41467-023-36288-4>.